Physics of Plasmas

Test particle simulation of direct laser acceleration in a density-modulated plasma waveguide

Cite as: Phys. Plasmas **19**, 113104 (2012); https://doi.org/10.1063/1.4766166
Submitted: 29 July 2012 • Accepted: 22 October 2012 • Published Online: 08 November 2012

M.-W. Lin and I. Jovanovic

View Online Export Citation CrossMark

ARTICLES YOU MAY BE INTERESTED IN

A particle-in-cell code comparison for ion acceleration: EPOCH, LSP, and WarpX
Physics of Plasmas **28**, 074505 (2021); https://doi.org/10.1063/5.0053109

Particle acceleration in relativistic laser channels
Physics of Plasmas **6**, 2847 (1999); https://doi.org/10.1063/1.873242

Direct laser acceleration of electrons in the plasma bubble by tightly focused laser pulses
Physics of Plasmas **26**, 083101 (2019); https://doi.org/10.1063/1.5110407

Submit Today!
Physics of Plasmas
Special Topic: Plasma Physics of the Sun in Honor of Eugene Parker

AIP Publishing

© 2012 American Institute of Physics.

Test particle simulation of direct laser acceleration in a density-modulated plasma waveguide

M.-W. Lin and I. Jovanovic[a)]
Department of Mechanical and Nuclear Engineering, The Pennsylvania State University, University Park, Pennsylvania 16802, USA

(Received 29 July 2012; accepted 22 October 2012; published online 8 November 2012)

Direct laser acceleration (DLA) of electrons by the use of the intense axial electric field of an ultrafast radially polarized laser pulse is a promising technique for future compact accelerators. Density-modulated plasma waveguides can be implemented for guiding the propagation of the laser pulse to extend the acceleration distance and for the quasi-phase-matching between the accelerated electrons and the laser pulse. A test particle model is developed to study the optimal axial density modulation structure of plasma waveguides for laser pulses to efficiently accelerate co-propagating electrons. A simple analytical approach is also presented, which can be used to estimate the energy gain in DLA. The analytical model is validated by the test particle simulation. The effect of injection phase and acceleration of electrons injected at various radial positions are studied. The results indicate that a positively chirped density modulation of the waveguide structure is required to accelerate electron with low initial energies, and can be effectively optimized. A wider tolerance on the injection phase and radial distance from the waveguide axis exists for electrons injected with a higher initial energy. © *2012 American Institute of Physics*. [http://dx.doi.org/10.1063/1.4766166]

I. INTRODUCTION

One of the most challenging tasks facing the future development of accelerator technology is the realization of much greater acceleration gradients compared to those offered by standard radio frequency-based accelerator structures. Laser-driven acceleration is emerging as an attractive approach to considerably increase the acceleration gradients, thus reducing the size and cost of future accelerators for a variety of applications.[1] The concept of laser wakefield acceleration (LWFA) has been demonstrated through numerous recent experiments, is well understood,[2–4] and now presents a rapidly maturing technology. In the highly nonlinear regime of plasma wave excitation typical for LWFA, acceleration gradients of up to 100 GV/m level can be obtained. However, LWFA typically requires laser peak powers in the range of tens of TW to be efficient. Laser pulses of requisite pulse energies are currently produced by complex and relatively low repetition rate laser systems, limiting the performance and attractiveness of the LWFA technique for many applications in which high repetition rates are desirable.

Direct laser acceleration (DLA) represents a promising alternative to LWFA when only modest laser peak powers are available. In DLA, the powerful electromagnetic field of an ultrashort laser pulse is used to accelerate electrons directly, without the intervening plasma waves.[5] Inverse Cherenkov acceleration,[6] inverse free-electron laser acceleration,[7] vacuum beat wave acceleration,[8] and acceleration with applied external magnetic fields[9] are some of the schemes that have been proposed for DLA. Those techniques use linear or circularly polarized laser pulses. It has been recognized recently that the use of radially polarized laser pulses[10] could be more effective than the use of more common polarization states of light since a focused radially polarized pulse provides a direct axial acceleration field, along with the cylindrically symmetric radial field.[11–15] A focused radially polarized fs laser pulse with $\sim 10\,\mu$m diameter and pulse energy of order mJ produces an axial electric field of order tens of GV/m,[11] which is comparable to the usual acceleration gradient in LWFA. However, since diffraction limits the effective acceleration distance to approximately one Rayleigh range, scaling the laser power to hundreds of TW would be needed to obtain electron energies in the range of 100's of MeV,[14] suggesting the need for an effective beam guiding mechanism to increase the acceleration distance. With appropriate beam guiding, DLA retains the promise for operation with considerably lower peak powers, even those available from novel fiber lasers,[16] which are not subject to the average power limitations of the usual bulk solid-state lasers.

Guiding a radially polarized laser pulse in a preformed plasma waveguide has been proposed as a method to extend the acceleration distance in DLA.[17] In a plasma waveguide exhibiting an appropriate transverse plasma density profile, radially polarized laser pulses can propagate over extended distances, thereby providing the axial electric field to accelerate co-propagating electrons to much higher energies than those available from unguided DLA. However, the difference in the phase velocity of the laser pulse and the velocity of accelerated electrons results in dephasing. In this situation, electrons cannot be accelerated continuously and instead experience alternating acceleration-deceleration phases in their subsequent propagation, without achieving significant net energy gain. Thus, the phase matching between the electron beam and the accelerating axial field of

[a)]Electronic mail: ijovanovic@psu.edu.

 © 2012 American Institute of Physics

the laser pulse represents an important challenge for DLA, for which quasi-phase-matching (QPM)[18] has been proposed as a possible solution. QPM in DLA is based on guiding radially polarized laser pulses in plasma waveguides with "slow-wave" structures.[19] The periodic density structure in a plasma waveguide expands the axial field to several harmonics, similar to the process occurring in conventional electron acceleration in RF structures. In this way, electrons can be accelerated continuously along the waveguide by the harmonic axial field having a subluminal phase velocity.

Density-modulated plasma waveguides can be fabricated by the laser machining technique,[20] based on the igniter-heater scheme.[21] Machined plasma waveguides have been used to demonstrate quasi-phase-matched relativistic harmonic generation.[22,23] In DLA, electrons fall out of phase by π with respect to the co-propagating laser field over a dephasing length. Akin to the ubiquitous QPM used in nonlinear optics, realization of QPM of DLA can be achieved by arranging alternating layers of low- and high-density plasma along the beam propagation direction. The electrons gain more energy in the longer low-density regions than the energy they lose in the shorter high-density regions. This allows a net energy gain to be produced by breaking the symmetry between acceleration and deceleration phases. Using this picture, the analysis of QPM of DLA considers the dephasing length and the corresponding optimal length of plasma structures that maximize the electron energy gain. In an equivalent picture, spatial harmonics of the laser field expanded in density-modulated plasma waveguides can be considered.[18] The modulation period of plasma structure is continuously varied to optimize the DLA for various initial energies of the injected electrons. The axial density function used in the model is a square function, which is appropriate for describing the shape of density modulations produced by the laser machining technique.[20,22,23]

In this work, we consider the use of laser-machined plasma waveguides for DLA. A gas with a low atomic number Z (e.g., hydrogen or helium) is used as the gas target, and the igniter-heater scheme for plasma waveguide production is considered. When a transverse femtosecond igniter beam, exhibiting a spatially varying intensity pattern and being sufficiently intense to ionize the gas, is passed through the neutral gas target, plasmas with a relatively low electron density are produced where the laser intensity is sufficiently high. The waveguide is subsequently irradiated by another long (hundreds of ps) and energetic (hundreds of mJ) heater pulse in the transverse direction, which heats and fully ionizes the plasma to the highest ionization state through the inverse bremsstrahlung heating mechanism. The increased axial temperature allows the hydrodynamic expansion of plasma to take place from the center of this plasma column, lowering the on-axis electron density, and forming a proper density profile to guide laser pulses in the longitudinal direction a few ns later (following the stage of hydrodynamic expansion). A longitudinal distribution with alternating low-density plasma regions (the regions with a transverse plasma density profile resembling a waveguide) and high-density neutral gas regions is created, as illustrated in Fig. 1. Subsequently, when an intense 0.5-TW radially polarized laser

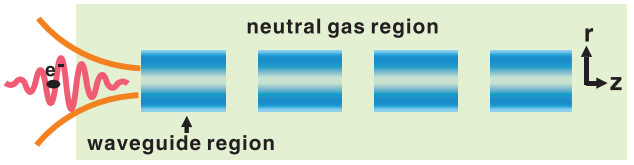

FIG. 1. Principle of quasi-phase-matched DLA with laser machined, density modulated plasma waveguide. The preformed waveguide regions and neutral gas regions become low- and high-density regions of the plasma that establish the QPM condition for DLA.

pulse with a peak intensity $>10^{17}\,\mathrm{W/cm^2}$ passes longitudinally though the plasma/gas structure, the front foot of the pulse ionizes the neutral gas in high-density regions. Throughout most of the laser pulse duration, the pulse experiences alternating low and high plasma density regions along the propagation distance. The low plasma density regions are those waveguide regions in Fig. 1, which have the density profile with a lowered on-axis electron plasma density. Since the plasma has reached its highest ionization state in these low plasma density regions, the electron density profile is not reshaped further during the passage of the DLA drive pulse. The high plasma density regions are fully ionized by the front foot of the drive laser pulse into an uniformly distributed plasma. As long as the neutral gas regions are shorter than the Rayleigh length for the guided mode radius, guiding of the laser pulse can be sustained with high efficiency over the waveguide length. The machining beam pattern, the heater beam energy, and the time delay between the heater pulse and the radially polarized drive pulse need to be optimized such that the axial structure (lengths of low- and high-density plasma regions) and the respective plasma densities in those regions of the plasma waveguide satisfy the QPM conditions for DLA.

Laser pulse energy depletion and/or beam defocusing in the neutral gas regions of the preformed plasma waveguide can render DLA ineffective. Ionization of gas atoms and the excitation of plasma wave by the laser pulse contribute to the depletion of laser pulse energy. The ionization process can also induce the refraction of laser pulse, which could further reduce the pulse intensity. When the laser pulse can fully ionize the low-Z gas by its front foot, i.e., within a few optical cycles, the pulse experiences an uniformly distributed plasma for most of its duration, rather than being considerably defocused by ionization-induced refraction.[24,25] Therefore, the evolution of the pulse transverse profile in the high-density gas region is still governed by the usual Gaussian beam diffraction. A fraction of the energy contained in the front foot of the laser pulse is consumed in ionizing the gas. The energy required to ionize a gas column of a given length can be compared with the energy contained in the front foot of the laser pulse to arrive with the characteristic depletion length caused by ionization of the neutral gas. Consider a laser pulse with a full-width at half-maximum (FWHM) Gaussian pulse duration τ_p and peak power P_0. The energy contained in the pulse for $t<\tau_0$ can be calculated as $E(-\tau_0)=\int_{-\infty}^{-\tau_0} P_0 \exp(-2t^2/\tau_0^2)\,dt$, with $\tau_0=\tau_p/\sqrt{2\ln 2}$ chosen as the characteristic time measured from the center of the pulse where the intensity is $e^{-2}\sim 0.135$ of the peak

intensity. The energy required to fully ionize a gas column can be estimated as $E_{i,tot} = n_a E_i V_{gas}$, where n_a is the gas atom density, E_i is the ionization potential of a single atom, and $V_{gas} = \pi r_0^2 L_{gas}$ is the volume of the gas column with radius r_0 and length L_{gas}. Here, $r_0 = 1.5 w_b$ defines the gas column radius where the intensity of the laser pulse with a beam radius w_b drops to $\sim e^{-2}$ of its peak intensity. For example, the energy $E(-\tau_0)$ enclosed in the front foot of a 20-fs, 0.5-TW laser pulse with $w_b = 8.5\mu$m can ionize a hydrogen gas column with length $L_{gas} \simeq 17.5$ mm, for $n_a = 1.25 \times 10^{19}$ cm^{-3} and $E_i = 13.6$ eV. Once the plasma is produced, the laser pulse energy can be depleted by exciting plasma waves. The pump depletion length $L_{pd} \simeq \frac{\omega^2}{\omega_p^2} \frac{c\tau}{a_0^2}$ characterizes the etching of the laser pulse energy in linear plasma wave excitation regime ($a_0 < 1$),[26] in which ω and ω_p are laser and plasma frequencies, c is the light speed, τ is the pulse length, and a_0 is the normalized vector potential of the laser pulse, defined as $a_0 = q_e E_{r,max}/m_e \omega c$. Here, q_e is the electron charge, $E_{r,max}$ is the maximum radial electric field, and m_e is the electron mass. For comparison, a 20-fs, 0.5-TW laser pulse ($a_0 = 0.275$), $L_{pd} \simeq 11.5$ mm is estimated with the electron density $n_e = n_a$ for a fully ionized hydrogen plasma. Thus, in this regime, the energy depletion of the laser pulse is dominated by the energy transfer to plasma wave excitation. L_{pd} calculated above is longer than the usual plasma waveguide produced in experiments[20,22] and considered here. In addition, the interlacing low- ($n_{e,L}/n_a$) and high-density ($n_{e,H} = n_a$) plasma regions in a density modulated plasma waveguide will further extend the pump depletion length L_{pd}. Therefore, the depletion of the laser pulse does not affect the DLA process significantly for plasma waveguide lengths in the range of 2–3 mm and electron plasma densities $\sim 10^{19}$ cm^{-3}, which are considered in this analysis.

In this paper, we describe the development of a test particle model and its application to study the QPM conditions for DLA in a laser-machined plasma waveguide. In Sec. II, closed-form description of a guided radially polarized laser pulse and the plasma waveguide is introduced, along with the relationships governing the electron acceleration in the test particle model. Numerical results and discussions of DLA performance are presented in Sec. III. The dephasing length and the optimal axial modulation structure for QPM of DLA in plasma waveguides are studied first. The results show that a positively chirped density modulation on the waveguide structure is required to satisfy optimal QPM conditions for accelerating electrons with lower initial energies ($\lesssim$20 MeV). The maximum energy gain can be calculated using an analytical formula, which reveals the parameters that dominate the acceleration process and is also validated by the test particle model. It is observed that the difference between the electron velocity and the laser group velocity can limit the effective acceleration distance in the waveguide for DLA with ultrashort laser pulses. The waveguide length also becomes another constraint that limits the energy gain when long laser pulses are utilized. The final energy gain electrons can acquire depends on their injected initial phase and radial position, limited by the QPM process and the finite laser spot size. For plasma waveguides with the modulation structure optimized according to the initial electron energy, the simulation results indicate that a greater tolerance for injection phase and radial injection distance from the waveguide axis exists for electrons with a higher initial energy. Finally, a discussion and the summary of the work are provided in Sec. IV.

II. DEVELOPMENT OF THE TEST PARTICLE MODEL

Our model for DLA is based on the dispersion relation for a radially polarized laser pulse guided in a preformed plasma waveguide.[17] Assuming the density along the radial direction of the waveguide increases quadratically, the dispersion relation under paraxial approximation is

$$\frac{\omega^2}{c^2} = k^2 + \frac{{\omega_{p0}}^2}{c^2} + \frac{8}{{w_0}^2}, \tag{1}$$

in which k is the wavenumber of the drive laser beam with wavelength λ, w_0 is the guided mode radius, $\omega_{p0} = n_{e0} q_e^2/\epsilon_0 m_e$ is the on-axis plasma frequency in the waveguide with electron density n_{e0}, and ϵ_0 is the vacuum permittivity. In the dispersion relation, the phase velocity of the drive laser pulse is $v_{ph} = \omega/k = c/\eta$ or

$$v_{ph} = c(1 - {\omega_{p0}}^2/\omega^2 - 8c^2/\omega^2 {w_0}^2)^{-1/2}, \tag{2}$$

and the refractive index η is

$$\eta = (1 - {\omega_p}^2/\omega^2 - 8c^2/\omega^2 {w_0}^2)^{1/2}. \tag{3}$$

The drive laser pulse propagates in the waveguide with a group velocity $v_g = dw/dk$ or

$$v_g = c(1 - {\omega_p}^2/\omega^2 - 8c^2/\omega^2 {w_0}^2)^{1/2}. \tag{4}$$

Using these governing relations, propagation of a radially polarized laser pulse in a plasma waveguide can be described. As is evident from these relations, propagation in a higher plasma density region or with a smaller beam mode radius results in a greater phase velocity, but a smaller group velocity.

When a radially polarized laser pulse is effectively guided in a plasma waveguide, the changes of amplitude and phase of the electric field due to beam diffraction can be neglected in its propagation. The electric field of a radially polarized pulse consists of a radial and axial component, $\mathbf{E} = \hat{r}E_r + \hat{z}E_z$, where E_r and E_z are in the following form:[11,17]

$$E_r = E_0 \theta (r/w_0) \exp[-(r/w_0)^2] \times \exp[-2\ln 2 (z - z_p)^2/L_p^2] \cos(\phi), \tag{5}$$

$$E_z = E_0 \theta^2 (1 - r^2/w_0^2) \exp[-(r/w_0)^2] \times \exp[-2\ln 2 (z - z_p)^2/L_p^2] \sin(\phi), \tag{6}$$

where $\theta = \lambda/\pi w_0$ is the beam diffraction angle, L_p is the pulse length in FWHM of a Gaussian longitudinal pulse

envelope centered at the axial position z_p, and ϕ is the phase. The characteristic field amplitude E_0 can be estimated for a given laser peak power P by

$$E_0 = \left(\frac{8c\mu_0 P}{\pi w_0^2 \theta^2}\right)^{1/2}. \quad (7)$$

For a laser pulse with peak power of $P = 0.5$ TW, $E_0 \simeq 86\,\mathrm{TV/m}$, the maximum radial amplitude $E_{r,max} = E_0\theta \simeq 1.1\,\mathrm{TV/m}$, and $E_{z,max} = E_0\theta^2 \simeq 77\,\mathrm{GV/m}$ with $w_0 = 8.5\,\mu$m and $\lambda = 800$ nm. Figure 2(a) depicts the transverse maximum electric field distribution. The cone-shape axial electric field peaks on beam axis, while the radial electric field is weak on axis and peaks at a radial position $r = w_0/\sqrt{2}$. The magnetic field associated with the laser pulse can be obtained from Faraday's Law ($\nabla \times \mathbf{E} = -\partial\mathbf{B}/\partial t$), and it is directed azimuthally as $B_\theta = (k/\omega)E_r$. Therefore, the azimuthal magnetic field can be obtained from the dispersion relation given in Eq. (1) as a function of radial field E_r as

$$B_\theta = \frac{\eta}{c}E_r, \quad (8)$$

where the refractive index η here accounts for the change of the magnetic field due to the presence of plasma and the effect of finite laser spot size. The phase is generally represented by $\phi = \omega t - kz$, or it can also be expressed by using the refractive index η as

$$\phi = \omega t - \frac{\omega}{c}\int \eta(z)dz. \quad (9)$$

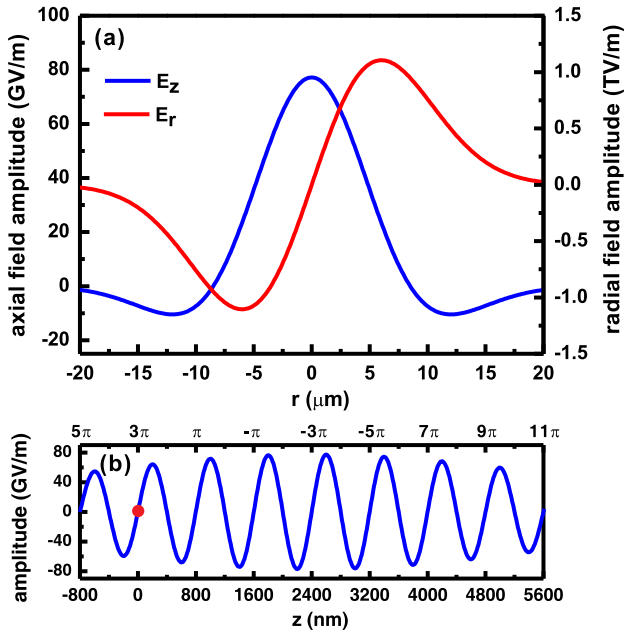

FIG. 2. (a) Axial E_z and radial E_r electric field transverse profiles of a guided radially polarized laser pulse with $w_0 = 8.5\,\mu$m. (b) An illustration of DLA of a electron (red point) by the axial field of a Gaussian laser pulse ($L_p = 6\,\mu$m). Initial positions (z) and corresponding initial phases are indicated on horizontal axes.

in the case where the medium is slowly varying in space, resulting in a variable axial refractive index $\eta(z)$.

In our model, the plasma electron density is expressed as a function of axial position

$$n_{e0}(z) = n_{e,L} + (n_{e,H} - n_{e,L}) \times H(z - \lambda_{L,n})[1 - H(z - \lambda_{m,n})], \quad (10)$$

where $n_{e,L}$ and $n_{e,H}$ are plasma densities in low- and high-density regions, $\lambda_{m,n} = \lambda_{L,n} + \lambda_{H,n}$ is the length of the nth modulation period composed of low- and high-density regions of lengths $\lambda_{L,n}$ and $\lambda_{H,n}$, respectively, and H is the Heaviside function used to describe the axial density changes. This on-axis plasma density distribution function is used to update the axial refraction index $\eta(z)$, on-axis plasma frequency $\omega_{p0}(z)$, and the laser pulse group velocity $v_g(z) = c\,\eta(z)$.

In the presence of electric and magnetic field, the relativistic equation of motion $d\mathbf{P}/dt = q_e(\mathbf{E} + \mathbf{v} \times \mathbf{B})$ governs the evolution of electron momentum $\mathbf{P}$, while the electron energy evolves as $m_e c^2 d\gamma/dt = q_e(\mathbf{v} \cdot \mathbf{E})$. Using $\mathbf{P} = \gamma m_e \mathbf{v}$ for simplification, equations for the electron position, momentum, and energy are summarized as follows:

$$\frac{dz}{dt} = P_z/\gamma m_e, \quad (11)$$

$$\frac{dr}{dt} = P_r/\gamma m_e, \quad (12)$$

$$\frac{dP_z}{dt} = q_e\{E_z + (P_r/\gamma m_e)[\ \eta(z)/c\ ]E_r\}, \quad (13)$$

$$\frac{dP_r}{dt} = q_e E_r\{1 - (P_z/\gamma m_e)[\ \eta(z)/c\ ]\}, \quad (14)$$

$$\frac{d\gamma}{dt} = (q_e/\gamma m_e{}^2 c^2)(P_z E_z + P_r E_r), \quad (15)$$

in which the electron angular momentum is ignored. For an electron co-propagating with the laser pulse at position z, the field amplitude it experiences depends on the instantaneous phase ϕ and the laser pulse position z_p. Since the electron also propagates with an axial velocity $v_z = P_z/\gamma m_e$ with respect to the wave of a phase velocity $v_{ph} = c/\eta$, the instantaneous phase change the electron experiences can be obtained by taking the time derivative of Eq. (9)

$$\frac{d\phi}{dt} = \omega\{1 - [\eta(z)/c\ ](P_z/\gamma m_e)\}. \quad (16)$$

The laser pulse position changes with time as

$$\frac{dz_p}{dt} = v_g(z_p), \quad (17)$$

where the laser pulse group velocity v_g is a function of axial position due to the axial plasma density modulation. The calculated ϕ and z_p are applied in Eqs. (5) and (6) in order to obtain the electric field amplitudes experienced by the electron. With appropriately assigned initial values, Eqs. (11)–(17) are numerically solved using the fourth-order Runge-Kutta method.

Figure 2(b) shows the result of a sample calculation of the initial axial position and phase assigned for a test particle and the laser pulse for some typical parameters expected in DLA.

III. TEST PARTICLE SIMULATION RESULTS AND DISCUSSION

A. Dephasing length in DLA

The dephasing length for DLA of electrons in a plasma waveguide is examined first by the use of the analytical dispersion relation in Eq. (1). For an electromagnetic wave of frequency ω and wave vector k_l and an electron with velocity v_e co-propagating with the laser pulse, a wave vector $k_e = \omega/v_e$ can be assigned to the electron, which can be used to directly estimate the phase mismatch. The dephasing length is defined as $L_c = \pi/|k_l - k_e|$ and is equal to the distance over which the electron would fall out of phase with respect to the electromagnetic wave by π. L_c is shorter in higher plasma density regions and for electrons with a lower kinetic energies because of the greater difference between the wave phase velocity v_{ph} and the electron velocity v_e. Figure 3 shows the dependence of dephasing length on electron energy for three different plasma electron densities with mode size $w_0 = 8.5\,\mu$m and laser wavelength $\lambda = 800$ nm. Unless specifically mentioned, this mode size and laser wavelength are used in the remainder of the simulations described here. Plasma densities chosen for the simulation and shown in Fig. 3 are typical for previous experimental studies of hydrogen plasmas.[20,22] In Fig. 3, dephasing lengths in high-density plasma regions can be shorter than 100 μm, which is relatively short compared to the Rayleigh length $z_r = \pi w_0^2/\lambda$ of a guided laser pulse in a plasma waveguide. For instance, $z_r \approx 284\,\mu$m for w_0 and λ chosen above. As a result, the short dephasing lengths in high-density regions of the density-modulated plasma waveguide could be considered as favorable for maintaining the waveguiding effect.

The dephasing length L_c shown in Fig. 3 is a function of the electron kinetic energy. However, as the electron is accelerated or decelerated by the field, the change of its velocity results in the change of the instantaneous dephasing length. This effect is more prominent for lower kinetic energies ($\lesssim$20 MeV). One can define the effective dephasing length L_d as the average of the instantaneous dephasing lengths over the entire acceleration/deceleration distance. To illustrate the use of the effective dephasing length L_d, electrons with several initial kinetic energies ($T_0 = 5$ MeV, 15 MeV, 40 MeV, and 100 MeV) are launched into a uniform (unmodulated) plasma waveguide. Figures 4(a) and 4(b) show the dependence of energy gain ΔT on axial distance for constant on-axis plasma density n_{e0} set to $n_{e,L} = 2.5 \times 10^{18}\,\mathrm{cm}^{-3}$ and $n_{e,H} = 1.25 \times 10^{19}\,\mathrm{cm}^{-3}$, respectively. L_d is defined as the acceleration distance at which the energy gain no longer increases with propagation. The following parameters are chosen for the calculation shown in Fig. 4: initial electron position $z_0 = 0$ and $r_0 = 0$, initial radial momentum $P_{r0} = 0$, initial pulse position $z_{p0} = 2.4\,\mu$m, and $\phi_0 = 3\pi$, as shown in Fig. 2(b). The initial axial momentum P_{z0} and the gamma factor γ_0 are determined from the initial kinetic energy. A 0.5-TW laser pulse with pulse length $L_0 = 6\,\mu$m is considered. Compared to the values of L_c in Fig. 3, L_d is generally longer for lower electron kinetic energies ($\lesssim$40 MeV) and approximately equal to L_c for higher electron energies ($\gtrsim$40 MeV). Take $T_0 = 5$ MeV electron for example, $L_c \approx 67\,\mu$m in Fig. 3, but the corresponding $L_d \approx 96\,\mu$m in

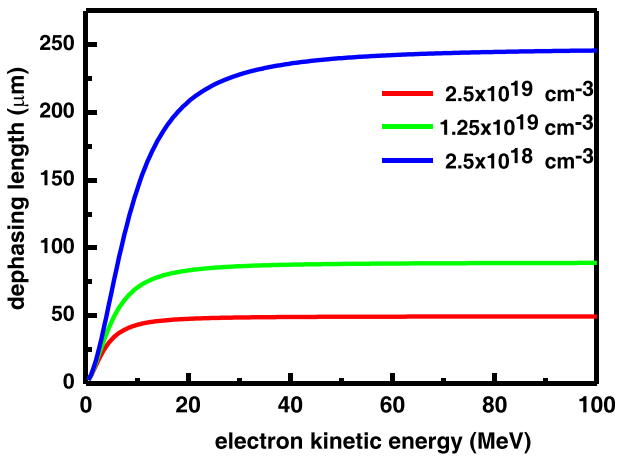

FIG. 3. Dependence of the dephasing length L_c on electron kinetic energy for $n_e = 2.5 \times 10^{18}\,\mathrm{cm}^{-3}$, $1.25 \times 10^{19}\,\mathrm{cm}^{-3}$, and $2.5 \times 10^{19}\,\mathrm{cm}^{-3}$ with $w_0 = 8.5\,\mu$m.

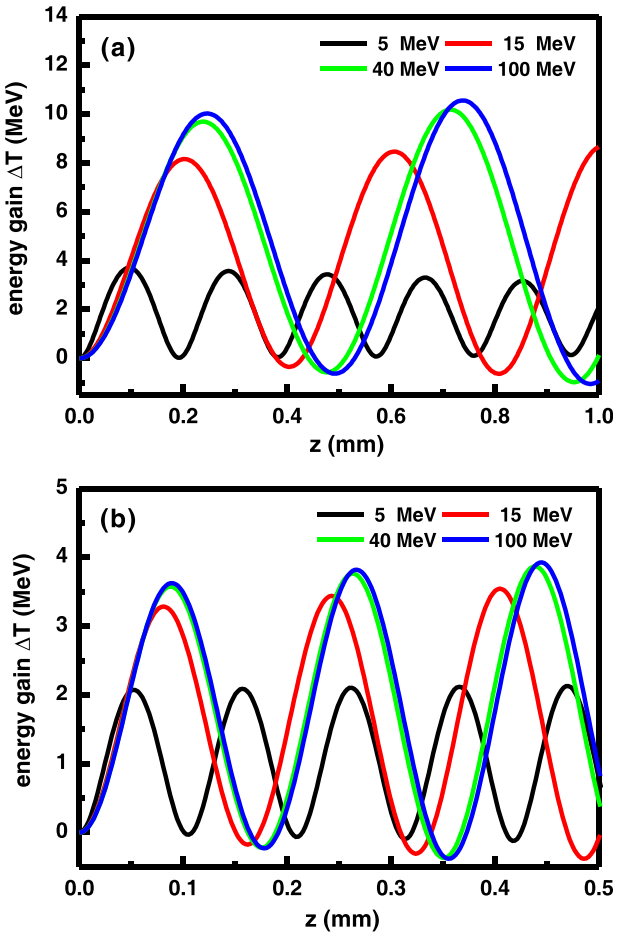

FIG. 4. Dependence of the electron energy gain ΔT on the propagation distance z at $n_e =$ (a) $2.5 \times 10^{18}\,\mathrm{cm}^{-3}$ and (b) $1.25 \times 10^{19}\,\mathrm{cm}^{-3}$ for electrons with $T_0 = 5$ MeV, 15 MeV, 40 MeV, and 100 MeV in uniform plasma waveguides.

Fig. 4(a). On the other hand, $L_c \approx L_d \approx 245\,\mu$m for $T_0 =$ 100 MeV electrons. The obtained effective dephasing lengths L_d in Fig. 4 help to set up the optimal plasma structure for QPM of DLA. As expected, L_d is shorter in Fig. 4(b) due to higher density $n_{e,H}$, which is consistent with the change of L_c in Fig. 3. Moreover, it can be observed that the amplitude of oscillating energy gain ΔT increases with the electron axial position. Since high-energy electrons can propagate faster than the laser pulse in plasmas, the increasing amplitude as a function of the electron axial position in this example reveals that electrons experience fields associated with the back and the central region of the laser pulse envelope. This difference in propagation velocities between electrons and laser pulses results in a walk-off effect in DLA, which would limit the electron energy gain for DLA driven by shorter laser pulse durations, as later discussed in this work.

B. Chirped density modulation for QPM of DLA

Since the dephasing length varies as a function of electron energy, QPM of DLA can be optimized by using variable modulation structures and electron densities in the plasma waveguide. We illustrate this by using electron densities $n_{e,L} = 2.5 \times 10^{18}\,\text{cm}^{-3}$ and $n_{e,H} = 1.25 \times 10^{19}\,\text{cm}^{-3}$ for low- and high-density regions of the waveguide, respectively. Figure 5(a) shows the dependence of the kinetic energy gain on the electron axial position in waveguides with constant density modulation periods equal to the effective dephasing lengths L_d obtained in Fig. 4. The result indicates that efficient quasi-phase-matched DLA utilizing constant density modulation period can only be achieved for electrons having higher initial kinetic energies ($T_0 = 40$ MeV and 100 MeV in this example), since for higher electron energies ($\gtrsim$40 MeV), further increase of electron energy does not significantly change the dephasing length, as shown in Fig. 3. In contrast, electrons with initial energies $T_0 = 5$ MeV and 15 MeV cannot be accelerated effectively in a waveguide with constant density modulation period. Even with an apparent energy gain in the first several periods for electrons of $T_0 = 15$ MeV, phase mismatch accumulates with distance and eventually leads to the acceleration process falling out phase. The rapid change of dephasing length for electrons starting with $T_0 = 5$ MeV causes the acceleration with constant density modulation period to be entirely ineffective.

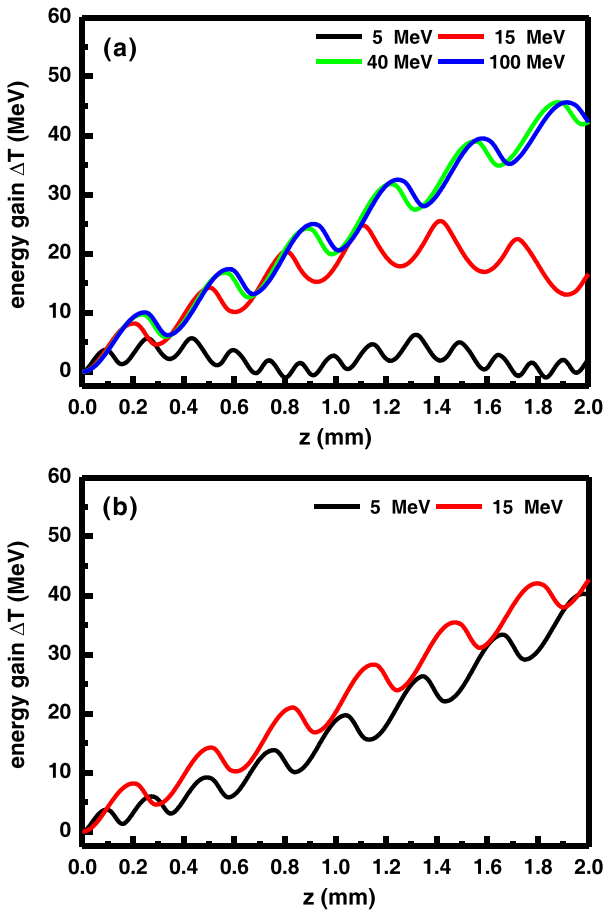

FIG. 5. Dependence of electron energy gain ΔT on propagation distance z for electrons with $T_0 = 5$ MeV, 15 MeV, 40 MeV, and 100 MeV in plasma waveguides with (a) constant and (b) chirped (only for $T_0 = 5$ MeV and 15 MeV) density modulations. The other parameters are given in the text.

Positively chirped density modulation (gradual increase in density modulation period) is required for low initial electron energies in order to better meet the QPM condition that rapidly changes with increasing electron energy. This approach to reduce the trapping threshold can be considered as an alternative to the previously proposed ramping up the electron density in the laser pulse propagation direction.[27] In Fig. 5(b), the result of the simulation of QPM DLA is shown for an aperiodic plasma modulation period, using the same parameters as in Fig. 5(a) and low electron initial energies ($T_0 = 5$ MeV and 15 MeV). The variation of the length of modulation regions used in the simulation is summarized in Table I. It is particularly important to carefully tune the plasma structure modulation length in the first few sections of the waveguide, so that low-energy electrons can continue to reach the acceleration phase. The modulation length is also increased according to the increase in electron energy and converges to dephasing length L_c for higher electron energies. We approximate each section length with $L_d = (L_{c,i} + L_{c,f})/2$, i.e., the average of dephasing length $L_{c,i}$ corresponding to the initial electron kinetic energy $T_{0,i}$ of that section, and the dephasing length $L_{c,f}$, corresponding to the approximated final kinetic energy $T_{0,f}$ after acceleration over $L_{c,i}$. An example of this approximation is provided for the first low-density section with the initial electron energy of $T_0 = 5$ MeV. According to Fig. 3, $L_{c,i} \approx 67\,\mu$m for $T_{0,i} = 5$ MeV. $T_{0,f}$ can be estimated by $T_{0,f} \approx C_e q_e E_{z,max} L_{c,i} = 8.3$ MeV, where C_e is defined as a

TABLE I. Assigned lengths, $L_{d,L}$ and $L_{d,H}$ (in μm), for low- and high-density regions in each section of the plasma waveguide providing optimal QPM conditions for DLA of electrons with initial energies $T_0 = 5$ MeV and 15 MeV shown in Fig. 5(b).

		Index of the modulation period							
T_0		1	2	3	4	5	6	7	8
5 MeV	$L_{d,L}$	100	120	150	180	210	220	230	240
	$L_{d,H}$	70	70	70	80	80	90	90	90
15 MeV	$L_{d,L}$	210	220	240	240	240	240	240	240
	$L_{d,H}$	80	80	90	90	90	90	90	90

factor for the half-cycle average of the electric field amplitude that changes within the dephasing length and is calculated as

$$C_e = \int_0^{\pi} \sin(\phi) d\phi/\pi \simeq 0.637. \tag{18}$$

$L_{c,f} \approx 120\,\mu$m, in accordance with $T_{0,f}$. Then, $L_d \approx 94\,\mu$m, or it is sufficiently accurate to set this L_d to $100\,\mu$m for convenience, as done in the first acceleration section $L_{d,L}$ for $T_0 = 5$ MeV in Table I. Using this method to estimate the lengths $L_{d,L}$ and $L_{d,H}$ in the chirped plasma waveguide, efficiency of QPM in DLA can be considerably improved.

C. Estimation of electron energy gain

As the laser pulse propagates in the plasma waveguide, the presence of plasma and the guiding effect reduces the laser pulse group velocity v_g, as shown in Eq. (4). For $n_e = 2.5 \times 10^{18}\,\text{cm}^{-3}$, $v_g \simeq 0.9984c$, corresponding to electron kinetic energy $T = 8.5$ MeV. When DLA utilizes an ultrashort laser pulse, energetic electrons initially at the back of the laser pulse can overtake the laser pulse even over modest distances, leading to the walk-off effect, which limits the effective acceleration distance. In this situation, we denote the effective acceleration distance as L_a and can consider it to be proportional to the pulse duration τ_p (or pulse length L_p). Increasing the pulse duration would reduce the field amplitude as $E_{z,max} \propto P^{1/2} \propto \tau_p^{-1/2}$ at constant pulse energy. The electron energy gain $\Delta T \propto q_e E_{z,max} L_a \propto \tau_p^{1/2}$; therefore, a longer pulse duration is more desirable for higher energy gain in DLA when the acceleration length is limited by the temporal walk-off. On the other hand, when waveguide length L_{wg} limits the effective acceleration distance, the energy gain ΔT scales as $\Delta T \propto q_e E_{z,max} L_{wg}$, and a shorter pulse duration is desirable.

Several correction factors should be considered in the estimation of energy gain ΔT when using this simulation method for QPM DLA. The first correction is associated with the variation of the electric field the electrons experience due to the difference between the electron velocity and laser group velocity, resulting in electrons sampling the field at various points of the laser pulse envelope. In the case when an electron with a velocity v_e co-propagates with a Gaussian laser pulse with a pulse length of L_p, the axial acceleration field envelope the electron would experience along the propagation direction z can be represented as

$$\text{env}(z) = E_{z,max} \exp[-2\ln 2 (z/L_{en})^2]. \tag{19}$$

The effective envelope width L_{en} is related to the laser pulse length L_p by

$$L_{en} = \frac{v_e}{v_e - v_{g,avg}} L_p, \tag{20}$$

where $v_{g,avg}$ is the laser group velocity averaged over distance z. In a density-modulated plasma waveguide composed of high-density regions of length $L_{d,H}$ and low-density regions of length $L_{d,L}$, $v_{g,avg}$ is

$$v_{g,avg} = \frac{L_{d,L} v_{g,L} + L_{d,H} v_{g,H}}{L_{d,L} + L_{d,H}}, \tag{21}$$

where $v_{g,L}$ and $v_{g,H}$ are the laser pulse group velocities in low- and high-density regions, respectively. As shown in Eq. (19), the walk-off effect can expand the laser pulse envelope to a dimension comparable to the length of the plasma waveguide. The electrons that experience a symmetrically distributed acceleration (laser field) envelope with respect to the waveguide dimension would acquire a maximum energy. The average amplitude of the field envelope can be defined as

$$\begin{aligned} C_{\text{env}} &= \frac{2}{L_{wg}} \int_0^{L_{wg}/2} \exp[-2\ln 2 (z/L_{en})^2]\, dz \\ &= \frac{1}{L_{wg}} \sqrt{\frac{\pi}{c'}} \text{erf}(\sqrt{c'} a'), \end{aligned} \tag{22}$$

with

$$c' = 2\ln 2 / L_{en}^2 \text{ and } a' = L_{wg}/2. \tag{23}$$

The second correction factor we define is due to the alternating acceleration and deceleration of electrons in the QPM process, which also reduces the DLA efficiency. This correction factor C_{qpm} can be defined as

$$C_{qpm} = \frac{L_{d,L} - L_{d,H}}{L_{d,L} + L_{d,H}} \tag{24}$$

when the electron accelerated over a length $L_{d,L}$ of the low-density region and decelerated over a length $L_{d,H}$ of the high-density region. The third correction factor, C_e in Eq. (18), associated with the axial field change over a length of the accelerating or decelerating section (equal to a dephasing length), should also be considered. With these correction factors, the energy gain ΔT for QPM DLA in a density-modulated plasma waveguide can be estimated as

$$\Delta T \simeq C_e C_{qpm} C_{\text{env}}\, q_e E_{z,max} L_{wg}. \tag{25}$$

For example, consider the electron with initial kinetic energy $T_0 = 40$ MeV ($v_e \simeq c$), plasma waveguide length $L_{wg} = 3$ mm, modulation lengths $L_{d,L} = 240\,\mu$m and $L_{d,H} = 90\,\mu$m for low- and high-density regions, respectively, with $n_{e,L} = 2.5 \times 10^{18}\,\text{cm}^{-3}$ and $n_{e,H} = 1.25 \times 10^{19}\,\text{cm}^{-3}$, and a 0.5-TW laser pulse with length $L_p = 6\,\mu\text{m}$ ($\tau_p \simeq 20$ fs). These parameters result in $v_{g,avg} \simeq 0.9976c$, $L_{en} \approx 2.5$ mm, $C_{\text{env}} \simeq 0.856$, $C_{qpm} \simeq 0.455$, and lead to energy gain of $\Delta T \simeq 57.4$ MeV.

To verify the effect of laser pulse duration on the estimated energy gain by Eq. (25) for quasi-phase-matched DLA, simulations with parameters the same as in the last example are performed for several pulse durations. For these simulations, the peak power and the electric field amplitude of the laser pulse decreases as the pulse duration increases, under the assumption that the laser pulse energy is fixed. The initial laser pulse position z_{p0} changes to $3.6\,\mu$m, so that test electron particles experience a symmetric acceleration field

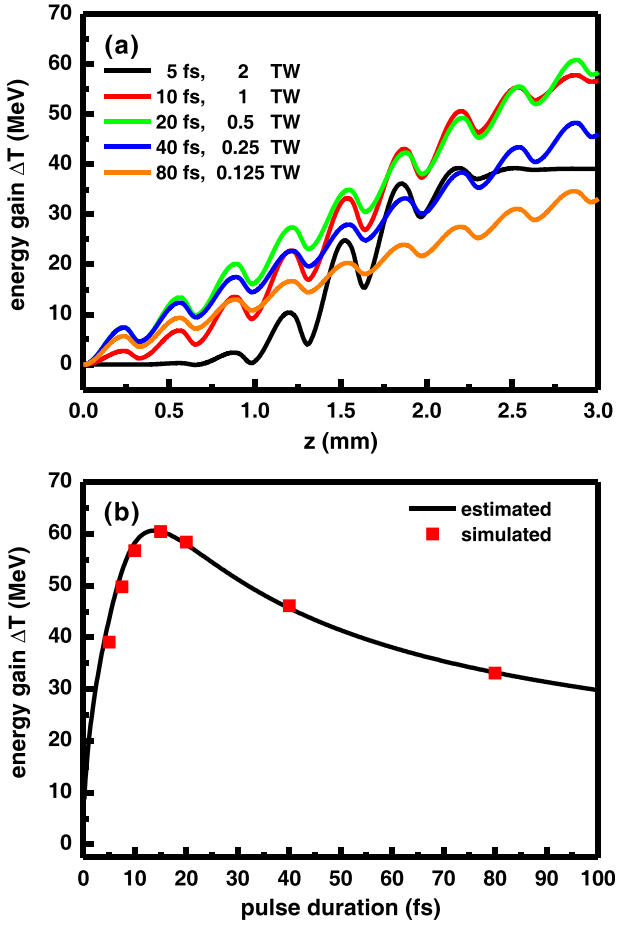

FIG. 6. (a) Dependence of the electron energy gain ΔT on propagation distance z in plasma waveguides for electrons of $T_0 = 40$ MeV with laser pulse durations $\tau_p = 5$ fs, 10 fs, 20 fs, 40 fs, and 80 fs. The other parameters are given in the text. (b) Comparison of estimated DLA electron energy gain ΔT from Eq. (25) to the results obtained by the test particle simulation.

envelope over a 3-mm long waveguide. Figure 6(a) shows the electron energy gain along the axial propagation distance for five different laser pulse durations. In the case of an ultrashort laser pulse ($\tau_p \leq 10$ fs), the peak power and field amplitude increase correspondingly, but the walk-off effect limits the acceleration at the initial and terminating sides of the waveguide, eventually resulting in energy gain reduction. Increasing the laser pulse duration ($\tau_p \geq 20$ fs) can reduce the walk-off effect; however, the decreased field amplitude and finite acceleration distance (L_{wg}) reduce the final energy gain as a result. Figure 6(b) shows the calculated energy gain ΔT from Eq. (25) as a function of laser pulse duration τ_p, with identical parameters as in Fig. 6(a), along with the results obtained by test particle model. The comparison of the two results in Fig. 6(b) indicates that the simulation matches well with the results predicted by Eq. (25), which can be used as an empirical relation for calculating the energy gain in DLA. As typical modern high-power fs laser facilities routinely generate pulses ≥ 30 fs, DLA should be operated in the regime in which the waveguide length L_{wg} limits the acceleration energy gain.

The time-dependent energy gain $\Delta T'$ for a flat-top laser pulse envelope has been discussed in Ref. 18

$$\frac{\Delta T'}{m_e c^2} \simeq 2\delta a_0 \left(1 + \frac{2\lambda_p^2}{\pi^2 w_0^2}\right)^{-1} \left(\frac{ct'}{w_0}\right), \tag{26}$$

where δ is the relative amplitude of the density modulation, $\lambda_p = 2c\pi c/\omega_p$ with $\omega_p^2 = \langle \omega_{p0}(z)^2 \rangle_z$ being the averaged axial plasma frequency over the propagation distance z, and t' is the elapsed time. The temporal walk-off between the electrons with velocities close to c and the laser pulse with a group velocity v_g' results in a pulse length dephasing time $t' \sim L_p/(c - v_g')$ for a given pulse length L_p. Consequently, the pulse length-limited energy gain $\Delta T'$ is

$$\frac{\Delta T'}{m_e c^2} \simeq 4\delta a_0 \left(\frac{L_p}{w_0}\right)\left(\frac{\lambda_p}{\lambda}\right)^2 \left(1 + \frac{2\lambda_p^2}{\pi^2 w_0^2}\right)^{-2}. \tag{27}$$

The energy gains estimated by Eqs. (25) and (26) are compared for $T_0 = 40$ MeV electron and a 0.5-TW laser pulse over $L_{wg} = 3$ mm. There is a good agreement between the energy gain obtained from Eq. (26) ($\Delta T' \simeq 50.1$ MeV) and that obtained from Eq. (25) ($\Delta T \simeq 57.4$ MeV). Further, we consider the pulse duration $\tau_p = 5$ fs in Fig. 6 and use Eq. (27) to compare the estimated energy gain when the temporal walk-off effect is significant. For $a_0 = 0.55$ (2-TW laser peak power) and $L_p = 1.5\,\mu$m with the remaining parameters identical to the immediately preceding case, Eq. (27) estimates the energy gain $\Delta T' \simeq 13.5$ MeV, which is only 32% of $\Delta T \simeq 42.1$ MeV obtained from Eq. (25). This significant difference results from the simplified dependence of energy gain $\Delta T' \propto L_p$ in Eq. (27) and from the difference between the calculated average laser pulse group velocities v_g in Eqs. (25) and (27). In Eq. (27), the pulse length $L_p = 1.5\,\mu$m results in electron acceleration over only 2 cycles. However, Fig. 6(a) indicates that the electron can be accelerated through approximately 5 cycles by a 5 fs pulse. The energy gain from the front and back of the pulse is not negligible. Moreover, the laser pulse group velocity v_g' in Eq. (27) is calculated from Eq. (4), while ω_{p0} is replaced by the averaged plasma frequency ω_p. With the same values for the electron densities ($n_{e,L}$, $n_{e,H}$) and the modulation length ($L_{d,L}$, $L_{d,H}$) as in Fig. 6, the calculated laser pulse group velocity v_g' yields $c - v_g' \simeq 0.0037c$. In contrast, $c - v_{g,ave} \simeq 0.0024c$ for $v_{g,ave}$ obtained from Eq. (21). As a result, the pulse length dephasing time for Eq. (27) is about 50% shorter than the one for Eq. (25), and $\Delta T'$ is further reduced because of the greater temporal walk-off mismatch. The definition of group velocity v_g' is more appropriate for a sinusoidal density modulation[18] than for a square modulation function, in which case Eq. (21) is more appropriate. In addition, the estimate of energy gain ΔT in Eq. (25) considers the laser with an Gaussian temporal pulse envelope, which is particularly important when DLA with ultrashort laser pulses is considered.

The correction factor C_{qpm} in Eq. (24) suggests that a greater difference between $L_{d,L}$ and $L_{d,H}$ could increase the DLA efficiency, which can be accomplished by increasing the plasma electron density for high-density regions, or further reducing the density in low-density regions. For example, when the density in high-density regions is increased to

twice its original value to $n_{e,H} = 2.5 \times 10^{19}\,\mathrm{cm}^{-3}$, the length of this region could be reduced to $L_{d,H} = 50\,\mu\mathrm{m}$ for 40 MeV electrons. With the remaining parameters for this calculation remaining the same as above, the C_{qpm} factor increases to 0.655 from 0.455, which is a 44% increase of the electron energy gain. To further study this improvement via the increase of $n_{e,H}$, simulations with parameters introduced in Fig. 5 and twice the original $n_{e,H}$ are performed (the density ratio $n_{e,H}/n_{e,L} = 10$ rather than 5 as in prior examples). Figure 7 shows the results when the calculation is performed in which the modulation lengths $L_{d,L}$ and $L_{d,H}$ are modified accordingly to meet the new QPM conditions with the doubled density of the high-density region, $n_{e,H}$. When compared to the results in Fig. 5, a 25%–50% increase of the electron energy gain can be obtained by doubling the high-density $n_{e,H}$. However, creating the plasma waveguides with a larger density ratio $n_{e,H}/n_{e,L}$ is experimentally more challenging.

D. Radial and out-of-phase electron injection

The simulation described in previous sections focus on studies of the acceleration of electrons fulfilling the optimal QPM conditions for DLA. In reality, the final energy gain electrons could acquire in DLA also depends on their initial axial and radial position relative to the laser field. The sinusoidally distributed axial field shown in Fig. 2(b) would accelerate electrons within initial phases of $n\pi$ to $(n+1)\pi$, where n is an odd integer, but decelerate those injected in a different phase. Whether electrons gain or loss energy is determined both by the injection phase and by the phase change of the electric field providing the accelerating force in the subsequent propagation. When the phase change is a function of axial position, only the electrons that remain in the acceleration phase would acquire high energy. The electrons could still accumulate energy gain despite falling into deceleration phases in parts of the DLA process, but this energy gain varies as a function of the total acceleration gradient sampled by electrons over the entire acceleration length.

By assigning various initial axial positions z_0 and related phases ϕ_0 along the central axis to test electrons, the size of the axial acceleration region can be investigated. Figure 8 shows the final electron energy gain ΔT as a function of initial phase ϕ_0 for four different initial kinetic energies T_0 with the optimal density modulations introduced in Fig. 5. The results indicate that the axial acceleration region increases its width with initial energy, which reflects the variation of the dephasing length with electron energy. For the case of $T_0 = 5$ MeV, most of the electrons injected into sub-optimal phase cannot be accelerated to the desired kinetic energy for meeting the QPM condition of the density-modulated structure optimized for a single injection phase, resulting in a narrow acceleration region. Particles with $\Delta T \sim 0$ in Fig. 8 experience rapid energy oscillation along the propagation distance, but cannot accumulate energy gain. In contrast, electrons with $T_0 = 100$ MeV experience a periodic energy gain as a function of initial phase. Note that the acceleration region shifts $\pi/2$ from the initial acceleration region. For example, electrons with initial phase $\phi_0 = 2.5\pi - 3\pi$ decelerate initially, but enter acceleration phases later in the process. The process is reversed when $\phi_0 = 3.5\pi - 4\pi$. The hump in the energy gain in the phase region $\phi_0 = 2.2\pi - 2.5\pi$ for $T_0 = 15$ MeV is a result of rapidly changing acceleration-deceleration processes as the particles propagate along the waveguide, with some kinetic energy still accumulated at the end of the process.

The finite laser mode size limits the radial size of the acceleration region.[18] The field distribution shown in Fig. 2(a) indicates that an off-axis electron experiences a reduced axial field amplitude. As a result, electrons at greater radial positions cannot be accelerated to the kinetic energies of on-axis electrons in a density-modulated plasma waveguide optimized for acceleration of on-axis electrons. Since the dephasing length (Fig. 3), changes rapidly in low-energy regions, off-axis electrons cannot continuously match the QPM condition provided by the plasma structure, and the radial acceleration region is further reduced. The radial field also induces a transverse force, Eq. (14), which focuses or defocuses electrons as they experience the change of phase

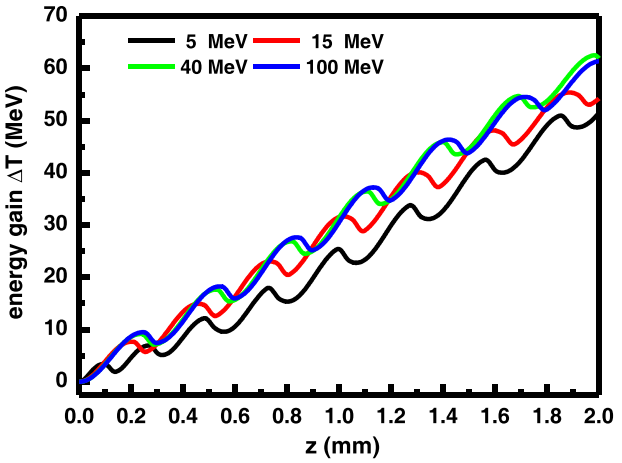

FIG. 7. Dependence of the electron energy gain ΔT on propagation distance z for electrons with $T_0 = 5$ MeV, 15 MeV, 40 MeV, and 100 MeV, with density ratio $n_{e,H}/n_{e,L} = 10$ in the plasma waveguide. The other parameters are given in text.

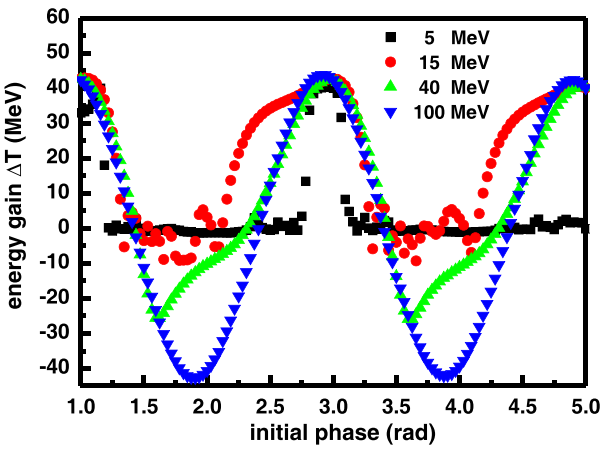

FIG. 8. Final electron energy gain ΔT as a function of electron initial phase ϕ_0 for electrons of $T_0 = 5$ MeV, 15 MeV, 40 MeV, and 100 MeV. The other parameters are the same for optimal density modulations in Fig. 5.

of the drive pulse.[18] The transverse force would be inhibited if the electron has a higher energy so that the axial velocity v_z becomes closer to c. The additional refractive index $\eta(z)$ term suggests that the radial force would become larger in a plasma than in the vacuum. Equations (5) and (6) for the electric field imply that the axial and radial forces are out of phase by $\pi/2$. Off-axis electrons in the optimal axial acceleration phase ($\phi_0 = \pi$) also experience a maximum radial defocusing force. To test the observations made above, a simulation of the transverse motion is performed, with electrons of $T_0 = 40$ MeV launched from several selected initial radial positions r_0, with corresponding parameters as introduced in Fig. 5(a). Figure 9(a) shows the deviation of the radial position along the propagation distance. Because of the QPM process, electrons remain primarily in the defocusing phase, leading to gradual radial divergence along the propagation distance. In this simulation, the radial field peaks at $r = w_0/\sqrt{2} \approx 5.8\,\mu$m. The final radial divergence depends on the initial radial position r_0 and is related to the radial field distribution. The maximum divergence shifts to $r_0 = 8\,\mu$m due to the lower axial velocity v_e by the reduced axial force in the outer region of the waveguide.

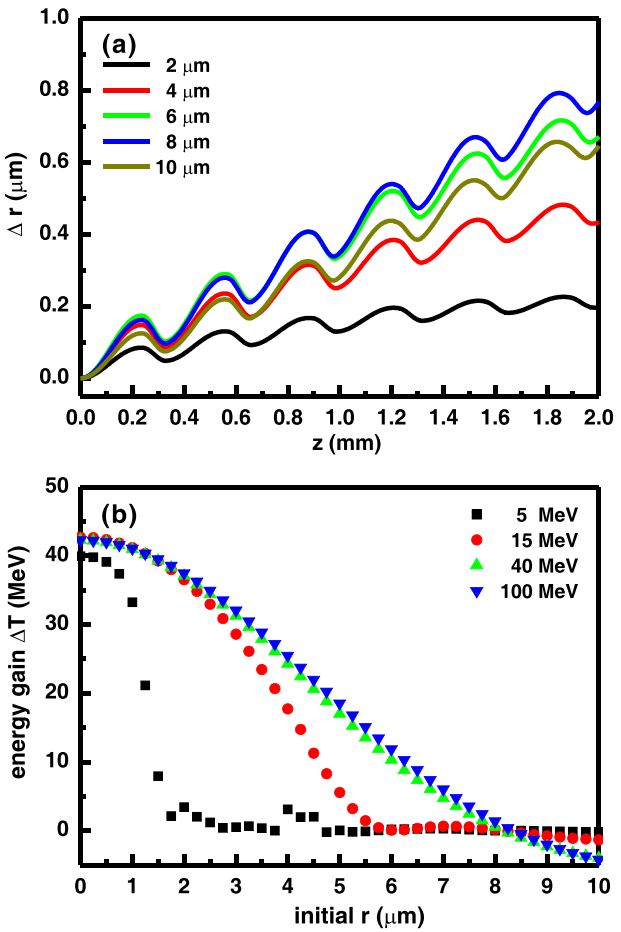

FIG. 9. (a) Dependence of the electron radial position shift Δr on the propagation distance z for electrons with $T_0 = 40$ MeV, with initial radial positions $r_0 = 2\,\mu$m, $4\,\mu$m, $6\,\mu$m, $8\,\mu$m, and $10\,\mu$m. (b) Final electron energy gain ΔT as a function of electron initial radial position r_0 for electrons of $T_0 = 5$ MeV, 15 MeV, 40 MeV, and 100 MeV and 2-mm long plasma waveguide. The other parameters are the same for optimal density modulations in Fig. 5.

To investigate the features of the radial acceleration region, test electrons are assigned various initial radial positions r_0, with the remaining simulation parameters identical to those in Fig. 5. Figure 9(b) shows the final electron energy gain ΔT as a function of the initial radial position r_0 for four different initial kinetic energies T_0. The results indicate that the radial acceleration region is narrower for lower initial electron energies. The lower axial field in the outer radial region fails to accelerate electrons to sufficiently high kinetic energies that can be consistent with the QPM condition as established by the waveguide plasma structure. The negative final energy gain in the radial region with $r \gtrsim 8\,\mu$m for $T_0 = 40$ MeV and 100 MeV corresponds to the reversed axial field direction as $r > w_0 = 8.5\,\mu$m. Therefore, the radial acceleration region is inherently restricted to the beam (or guided mode) dimension, regardless of the QPM condition and initial electron energy. The results presented in this section show that the axial and radial acceleration regions in an optimized plasma structure are larger for electrons injected with a higher initial energy.

IV. CONCLUSION

A detailed study of the DLA process has been presented, with a goal to understand its potential for use in developing future compact particle accelerators. A test particle model has been described, which reveals that a positively chirped density modulation of the waveguide structure is required, especially for DLA with low electron kinetic energies ($\lesssim$20 MeV). For such low injected electron energies, DLA dephasing length changes rapidly with the increased electron energy. Therefore, the plasma structure should be varied accordingly, so that electrons can remain in the acceleration phase over the propagation distance.

Energetic electrons ($\gtrsim$10 MeV) can propagate faster than the laser pulse in the plasma waveguide. The difference between the electron velocity and the laser group velocity leads to the temporal walk-off effect, which expands the laser pulse envelope to an equivalent acceleration field envelope with a dimension comparable to that of the plasma waveguide. For DLA driven by an ultrashort laser pulse, the electrons can overtake the laser pulse, so that the effective acceleration distance is limited. When a long laser pulse is used such that the width of effective acceleration envelope becomes lager than the length of the plasma waveguide, the acceleration distance is then limited by the waveguide length even though the walk-effect is reduced. Making the width of the effective acceleration envelope closer to the waveguide length should enable a higher energy gain if this laser pulse duration is practically achievable in experiments. A analytical formula is proposed to estimate the final energy gain, and it considers the correction factors for the average of field change over a dephasing length, the efficiency of QPM process, and the average amplitude of the acceleration field envelope. The correction factor for the QPM efficiency also suggests that the energy gain can be increased by increasing the density ratio between the high- and low-density regions. This formula can be used as an empirical relation for

estimating the energy gain in DLA, as its results are verified by the test particle simulations.

The DLA energy gain also depends on the injected initial axial (related to the initial phase) and radial position of electrons. Only electrons having proper initial phases can continuously stay in the acceleration phase of QPM process to accumulate significant final energy gain. Since the modulation structure of a plasma waveguide is optimized according to the initial energy of on-axis electrons, the finite laser mode size limits the radial acceleration region such that off-axis electrons cannot be accelerated consistently with the QPM condition. The radial field also induces a transverse force, defocusing the off-axis electrons. As a result, the accelerated off-axis electrons gradually diverge in radial position along the propagation distance. In summary, the simulation results indicate that larger axial and radial acceleration regions exist for electrons injected with a higher initial energy.

ACKNOWLEDGMENTS

This work has been supported by the Defense Threat Reduction Agency through Contract HDTRA1-11-1-0009.

[1]V. Malka, J. Faure, Y. A. Gauduel, E. Lefebvre, A. Rousse, and K. Ta Phuoc, Nat. Phys. **4**, 447 (2008).
[2]T. Tajima and J. Dawson, Phys. Rev. Lett. **43**, 267 (1979).
[3]E. Esarey, C. B. Schroeder, and W. P. Leemans, Rev. Mod. Phys. **81**, 1229 (2009).
[4]V. Malka, Phys. Plasmas **19**, 055501 (2012).
[5]G. Malka, E. Lefebvre, and J. L. Miquel, Phys. Rev. Lett. **78**, 3314 (1997).
[6]W. D. Kimura, G. H. Kim, R. D. Romea, L. C. Steinhauer, I. V. Pogorelsky, K. P. Kusche, R. C. Fernow, X. Wang, and Y. Liu, Phys. Rev. Lett. **74**, 546 (1995).
[7]E. D. Courant, C. Pellegrini, and W. Zakowicz, Phys. Rev. A **32**, 2813 (1985).
[8]E. Esarey, P. Sprangle, and J. Krall, Phys. Rev. E **52**, 5443 (1995).
[9]K. P. Singh, Phys. Plasmas **11**, 3992 (2004); D. N. Gupta and C.-M. Ryu, *ibid.*, **12**, 053103 (2005).
[10]Q. Zhan, Adv. Opt. Photon. **1**, 1 (2009).
[11]Y. I. Salamin, New J. Phys. **8**, 133 (2006).
[12]Y. I. Salamin, Phys. Rev. A **73**, 043402 (2006).
[13]D. N. Gupta, N. Kant, D. E. Kim, and H. Suk, Phys. Lett. A **368**, 402 (2007).
[14]P. L. Fortin, M. Piche, and C. Varin, J. Phys. B **43**, 025401 (2010).
[15]K. P. Singh and M. Kumar, Phys. Rev. ST Accel. Beams **14**, 030401 (2011).
[16]J. Limpert, S. Hädrich, J. Rothhardt, M. Krebs, T. Eidam, T. Schreiber, and A. Tünnermann, Laser Photon. Rev. **5**, 634 (2011).
[17]P. Serafim, P. Sprangle, and B. Hafizi, IEEE Trans. Plasma Sci. **28**, 1155 (2000).
[18]J. P. Palastro, T. M. Antonsen, S. Morshed, A. York, and H. M. Milchberg, Phys. Rev. E. **77**, 036405 (2008); A. G. York, H. M. Milchberg, J. P. Palastro, and T. M. Antonsen, Phys. Rev. Lett. **100**, 195001 (2008); J. P. Palastro and T. M. Antonsen, Phys. Rev. E. **80**, 016409 (2009); B. D. Layer, J. P. Palastro, A. G. York, T. M. Antonsen, and H. M. Milchberg, New J. Phys. **12**, 095011 (2010).
[19]B. D. Layer, A. York, T. M. Antonsen, S. Varma, Y.-H. Chen, and H. M. Milchberg, Phys. Rev. Lett. **99**, 035001 (2007).
[20]M.-W. Lin, Y.-M. Chen, C.-H. Pai, C.-C. Kuo, K.-H. Lee, J. Wang, S.-Y. Chen, and J.-Y. Lin, Phys. Plasmas **13**, 110701 (2006).
[21]P. Volfbeyn, E. Esarey, and W. P. Leemans, Phys. Plasmas **6**, 2269 (1999).
[22]C.-C. Kuo, C.-H. Pai, M.-W. Lin, K.-H. Lee, J.-Y. Lin, J. Wang, and S.-Y. Chen, Phys. Rev. Lett. **98**, 033901 (2007).
[23]C. S. Liu and V. K. Tripathi, Phys. Plasmas **15**, 023106 (2008).
[24]R. C. Rae, Opt. Commun. **97**, 25 (1993).
[25]W. P. Leemans, C. E. Clayton, W. B. Mori, K. A. Marsh, P. K. Kaw, A. Dyson, C. Joshi, and J. M. Wallace, Phys. Rev. A. **46**, 1091 (1992).
[26]W. Lu, M. Tzoufras, C. Joshi, F. S. Tsung, W. B. Mori, J. Vieira, R. A. Fonseca, and L. O. Silva, Phys. Rev. ST Accel. Beams **10**, 061301 (2007).
[27]S. J. Yoon, J. P. Palastro, D. Gordon, T. M. Antonsen, and H. M. Milchberg, Phys. Rev. ST Accel. Beams **15**, 081305 (2012).